

Identification of Source of Oscillations in Apparent Sarcomere Length Measured by Laser Diffraction

Kevin Burton* and Andrew F. Huxley†

*MRC Muscle and Cell Motility Unit, King's College London, London WC2B 5RL, United Kingdom, and †Physiological Laboratory, Cambridge, CB2 3EG, United Kingdom

ABSTRACT The most widely used technique for dynamic estimates of sarcomere length in muscle is laser light diffraction. We have identified conditions under which artifactual oscillations can arise in apparent sarcomere length measured by this technique and report methods to reduce the effect. Altringham et al. (1984) first reported that the diffraction angle can exhibit one cycle of oscillation for each sarcomere length displacement of the illuminated portion of the fiber. We find that the amplitude of similar oscillations is strongly dependent on the intensity of light scattered from objects near the fiber and on the spacing between fiber and scatterer. The oscillations can be eliminated by minimizing scattered light and positioning the fiber a few millimeters from sources of scattering. A theoretical description shows that oscillations of this kind are expected from interference of scattered and diffracted light. Interference fringes were observed along the meridian of the pattern, and these moved during translation of either a fiber or a grating. The movement of fringes across the diffraction order shifts the centroid back and forth and, when associated with steady shortening, can give rise to "steps" and "pauses" in apparent striation spacing.

INTRODUCTION

The ability of striated muscle fibers to act as a diffraction grating when illuminated by light of optical wavelengths has allowed estimates of average sarcomere length to be made using the angle of the first order. Light diffraction is the most widely used method to estimate average striation spacing because, in part, of the ease with which the position of a diffraction order can be rapidly quantitated with simple optical elements. Illumination commonly is provided by a laser, which is a convenient and inexpensive source of monochromatic light that is usually highly collimated. The bright, highly coherent beam also produces diffraction orders that are intense in an absolute sense as well as relative to off-order light. The full dynamic range of most photodetectors thus can be used, and the signal-to-noise ratio is increased relative to measurements made with conventional light sources. The method, however, must be used with caution because errors in sampling mean striation spacing can arise when the diffractor is much thicker than the illumination wavelength, as is the case with single skeletal muscle fibers, thus giving rise to Bragg angle effects (Rüdel and Zite-Ferenczy, 1979b; Yeh et al. 1980; Baskin et al., 1981; Zite-Ferenczy et al., 1986; Huxley, 1990). Approaches to reducing such sampling errors have included varying the angle of incidence over a wide range (Rüdel and Zite-Ferency, 1979a; Lieber et al., 1984; Goldman and Simmons, 1984; Brenner, 1985; Burton and Baskin, 1986), estimating striation spacing using diffraction angles of two or more orders (Rüdel and Zite-Ferenczy,

1979b; Burton et al., 1989), or using a range of wavelengths or laser light of reduced coherence (Goldman, 1987). The high coherence of laser light also can result in interference between separate domains of striations of defined spacing and tilt. The resulting fringes contribute to fine structure in the order and can shift its centroid (Brenner, 1985; Sundell et al., 1986).

Efforts to correct for these sources of error have been motivated partially by controversial reports, originally based on laser diffraction measurements, in which striation spacing appeared to execute a series of steps and pauses as a single muscle fiber was released at constant velocity (Pollack et al., 1977; Granzier and Pollack, 1985). Although evidence using other methods to estimate striation spacing has been presented in support of these observations (Pollack, 1986; Pollack et al., 1988), it has been argued that several sources of uncertainty compromise these approaches (Altringham et al., 1984; Huxley, 1984, 1986). Altringham et al. (1984) reported oscillations in diffraction order centroid when striations were translated through the laser beam. Such oscillations, when superimposed on an otherwise constant velocity length change, resulted in apparent steps and pauses. No clear account of the origin of these oscillations was given, and we are not aware of similar reports.

We describe a characterization of oscillations of this type described by Altringham et al. (1984) and show that their amplitude can be controlled and easily reduced. We have identified the source of these oscillations and provide a theoretical description that accounts for their principal properties. They occur in active and passive fibers that are shortened, lengthened, or merely translated through the laser beam. Similar oscillations occurred when a plane grating was passed through the beam. Potential uses of the phenomenon are also considered. A preliminary account of this work has appeared in abstract form (Burton and Huxley, 1991).

Received for publication 18 November 1994 and in final form 23 March 1995.

Address reprint requests to Dr. Kevin Burton, Center for Light Microscope Imaging and Bio-technology, Carnegie Mellon University, 4400 Fifth Avenue, Pittsburgh, PA 15213-2683.

© 1995 by the Biophysical Society

0006-3495/95/06/2429/15 \$2.00

MATERIALS AND METHODS

Materials

Single fibers obtained from rabbit psoas muscle were used. Small strips of muscle were skinned in relaxing solution containing 0.5% Brij 35 detergent and either kept on ice and used within 1 week or glycerinated in 50% glycerol/50% relaxing solution and used within 1 month. The relaxing solution was (in mM): K⁺ propionate 70, Mg²⁺ Acetate 8, K₂EGTA 5, Na₂ATP 7, Imidazole 6, pH 6.8, at 0°C, ionic strength 100 mM. Activating solution was the same except that Ca²⁺-EGTA was added to produce a pCa of 4.0. Protease inhibitors (phenylmethylsulfonyl fluoride (0.1 mM), leupeptin (8 μg/ml), trypsin inhibitor (0.1 mg/ml)) were added to the skinning and storage solutions.

Apparatus

Segments of single fibers (60–100 μm in diameter and 2–3 mm long) were held in a small volume of solution (20–40 μl) in two ways. For experiments in which fiber length was to be varied, the fiber was attached to hooks via aluminum foil T-clips crimped onto the ends. The hook at one end was attached to a servomotor for controlling length and at the other end to a semiconductor strain gauge. For experiments in which fibers were to be translated through the laser beam at constant length, the clips were stuck to a 1-mm-wide strip of #0 coverslip (thickness ~100 μm) using Vaseline petroleum jelly as adhesive. One end of the strip of coverslip was affixed to the servomotor, and the other end was free. In those experiments in which a grating was used in place of a fiber, the grating was placed on the strip of coverslip in air. Temperature was usually maintained at 5 ± 0.1°C during an experiment by flowing a mixture of ethylene glycol and water (1:2) past the bottom of the chamber containing the experimental solution. The temperature of the coolant was controlled by flowing through a Peltier-cooled copper block. Temperature was measured by a small (200 μm) thermistor placed near the fiber. In the case of records longer than 0.1 s, flow was usually stopped during data acquisition to avoid optical effects arising from pressure pulses at 3 s⁻¹ produced by a peristaltic pump.

Optics

A fiber or grating was illuminated from below at a wavelength of 632.8 nm by a 5 mW HeNe laser (05 LHP 151, Melles Griot, Irvine, CA). The beam was reflected through the bottom of the chamber and onto the fiber by a front-surface mirror that could be rotated and translated to control the angle of incidence. A cylindrical lens focused the beam down to ~0.3 mm perpendicular to the fiber axis while the beam remained about 1 mm (full width at 1/e² = 0.8 mm) along the axis. A #0 coverslip was used to flatten the surface of the solution bathing the fiber to eliminate refraction artifact. Condensation on the cold glass surfaces in the path of the beam was prevented by a stream of cool, dry nitrogen gas arising from evaporation of liquid nitrogen (Sleep, 1990). For studies in which the diffracted light was monitored by a position-sensitive photodiode, a cylindrical lens placed above the fiber focused the diffracted light in the equatorial direction so that only meridional movements were significant. A pair of cylindrical lenses was used to pass and focus the light when the photodiode was moved relatively far from the fiber to increase sensitivity to movements of the diffraction order. A variable slit was placed in front of the photodiode with spacing adjustable from 0.1 mm to greater than the meridional dimension of the photodiode (3 cm).

Scattered light was produced in several ways. These included placing a thin layer of silicone rubber or epoxy resin in the path of the beam at the bottom of the experimental chamber, which was made to contain small irregularities (e.g. bubbles) that scattered light. Another approach was to place small, transparent dextran beads (5- to 80-μm diameter) on the bottom of the chamber. In many experiments, a glass filament (35-μm diameter) was placed on the bottom of the chamber perpendicular to the muscle fiber axis. The part of the laser beam intersecting the filament was refracted into a disk that provided a line of light along the meridian of the diffraction pattern. Because this scattered light was

spatially localized, it was easier than with the diffuse scatter of the other methods to distinguish movements of fringes resulting specifically from scattering. In some experiments, scatterers also were placed on the coverslip above the fiber at the surface of the solution. The separation between scatterer and fiber could be varied by raising and lowering either the chamber below, or coverslip above, the fiber. The fiber-scatterer separation could not be reduced to zero because of physical constraints of the system. In the case of a fiber riding on a coverslip, the minimum spacing was greater than the 100-μm thickness of the glass because the fiber was held up off of the glass by clips on either end, and care was required to avoid hitting the scattering material beneath the coverslip. The practical minimum separation between the top of the scatterers and bottom of the fiber, therefore, was ~130 μm. The thickness of scatterer and fiber also reduced the precision of this number. Vertical movement of the chamber was measured to within 10 μm using a dial gauge. The hooks could be positioned independently of these surfaces to align the fiber in the beam. Changes in amplitude and centroid of diffraction intensity were monitored either by using a position-sensitive photodiode (LSC 30D, United Detector Technology, Hawthorne, CA) or by visualizing the pattern on a screen. The active area of the photodiode was 3 × 0.4 cm. Outputs of current at either end of the photodiode were converted to voltage, and their difference divided by their sum was proportional to position for movements over the central 2 cm of the photodiode. The sum of the two outputs provided a measure of total irradiance at the photodiode. When the photodiode was positioned on the diffraction order, noise in the position signal was the equivalent of ~0.2–1.3 nm sarcomere length (peak-to-peak, 8 μm at the photodiode) over a bandwidth of 1 kHz and ~0.05–0.4 nm when a 100-Hz RC filter was used. The range mainly represents increased change in diffraction angle for a given movement at the photodiode as the photodiode was moved nearer to the fiber (distance = 113–810 mm). Signal-to-noise ratio was reduced at low intensity and decreased by a factor of four to five when the photodiode was positioned between diffraction orders.

The photodiode signal was amplified and then recorded on oscilloscopes or magnetic disk. The oscilloscope traces were either photographed onto Polaroid prints or transferred directly from a digital oscilloscope (8 bits, Gould Instruments #400) to a plotter (Hewlett-Packard Color-Pro). In some experiments, the signals were also digitized (12-bit resolution) onto disk using a computer. In several experiments, the pattern was imaged by a video camera and the data recorded onto magnetic tape.

Analysis

Expectations based on a theoretical description (Appendix) were calculated, and tests of its assumptions made using a Fortran program run on a VAX 4000-100. It was necessary to estimate the relative contributions of scattered and diffracted light for comparison of experiment to theory. These quantities were obtained by placing a slit on the diffraction order and measuring total intensity with the fiber alternately in and out of the laser beam. The version of the theory that uses a Gaussian intensity profile in the beam assumes that these quantities refer to the maximum intensity in the diffraction order. Although a narrow slit occasionally was used, it was more common to include the entire width of the order. In these cases, the "width" was assumed to be 5 SD of the Gaussian intensity distribution, at the edges of which the intensity falls to 4.4% of the peak. On this assumption, the ratio of scattered to diffracted light at the center of the order would be ~50% of the measured value. Video data were digitized onto computer from videotape using a frame-grabber for purposes of quantitation, and display and contrast enhancement was performed with software.

RESULTS

Dependence of oscillations on fiber translation

Using the first-order diffraction angle of a laser beam to estimate striation spacing during ramp shortening, the apparent change in spacing occasionally deviated from linearity

in an oscillatory fashion. These oscillations occurred irrespective of whether the fiber was active or relaxed, or released or stretched. It became apparent that these oscillations behaved as those described by Altringham et al. (1984), in whose work it was found that one cycle of oscillation was completed for every sarcomere length displacement of the illuminated portion of the fiber. In the case of a relaxed fiber, translation through the laser beam produced by displacement of one end could be estimated from the velocity of length change, the relative position along the fiber of the illuminated spot, and the assumption that the length change is distributed evenly along the fiber (Paolini et al., 1976; Goldman and Simmons, 1984). The calculated displacement at the center of the beam during the period of one oscillation was approximately equal to the sarcomere length estimated from the first-order diffraction angle (Fig. 1). Because both sarcomere length and the relative position of the beam along the fiber were altered by the length change, the period of oscillation changed slightly during the ramp (increased in the case of a stretch). The intensity of the first order exhibited oscillations at the same frequency as the centroid, but shifted by one-quarter cycle. As shown by Altringham and colleagues, the oscillation frequency could be altered by changing the rate of displacement of the illuminated portion of the fiber, for example, by illuminating a fiber near the fixed versus moving ends during length changes (Fig. 2). A more direct comparison was made by translating the entire fiber at constant length (Fig. 3 A). In this experiment, the rate of fiber translation was known precisely and a one to one relationship was observed between cycles of oscillation and displacement of striations.

The observed oscillations were not dependent on Bragg angle effects, but rather on the grating component of muscle fiber diffraction. This was demonstrated by translating a transmission grating (1.9- μm spacing) through the beam (Fig. 3, B and C). Oscillations were observed with similar properties to those using a muscle fiber, although frequently of smaller amplitude.

Identification of a source of oscillations

The amplitude was found to be a strong function of the separation (h) between the fiber and a source of scattered light. For the data of Fig. 1 A, scattering was produced by a thin layer of nominally transparent silicone rubber separating layers of glass that, in the case of these data, formed the bottom of the chamber. The cross section of the laser beam was visible at an angle to the beam as it passed through these layers and, hence, scattered light was present. As the chamber was lowered away from the fiber and h increased, the amplitude of oscillation generally decreased. Oscillations were apparent at small h , even though the scattering intensity was only $\sim 0.25\%$ of the diffraction intensity. A test of the dependence of oscillation amplitude on scattered light was provided by increasing the intensity of scattering by depositing small transparent beads (5- to 80- μm diameter) on the bottom of the chamber. In the records of Fig. 1 B, scattering

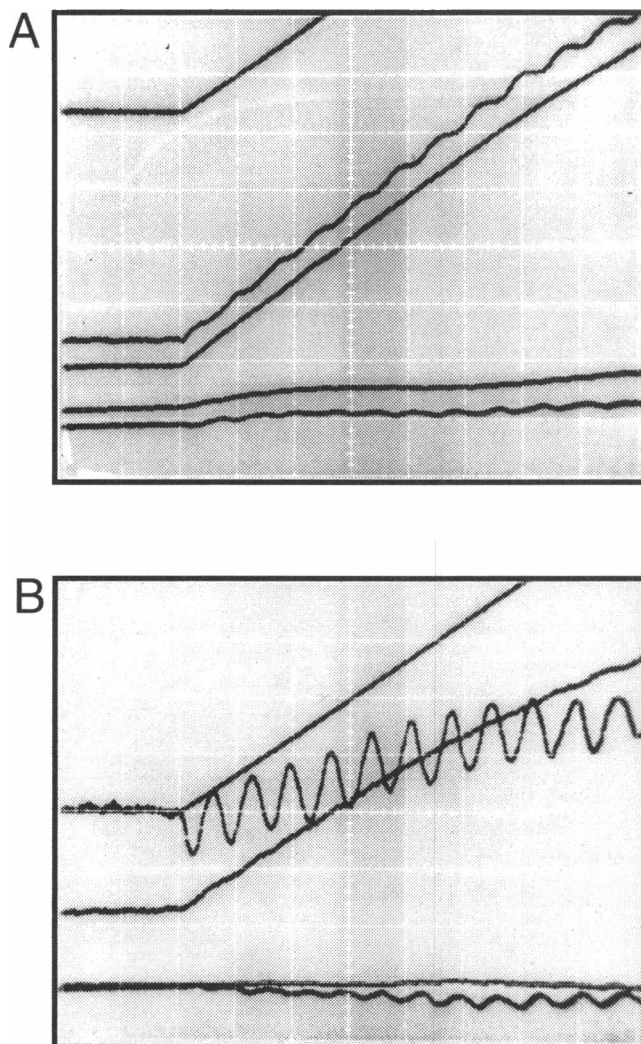


FIGURE 1 Dependence of oscillation amplitude on scattered light. Each panel shows records of fiber length (*top*), apparent striation spacing (*middle*), and intensity (*bottom*) during stretch of a relaxed fiber. Striation spacing and intensity are each represented by a pair of records, at ≈ 0.15 – 0.2 and 2 mm spacing (h) between fiber and scatterer, with the trace exhibiting larger oscillation recorded at lower h . The data were recorded in the presence of low scattering ($\approx 0.25\%$ of the intensity measured over the width of the order; see “Analysis” in Materials and Methods) in A and high scattering intensity ($\approx 4\%$) in B produced by 5- to 80- μm diameter transparent beads. One oscillation required about 0.034 s (1st full oscillation in B at $h \approx 0.2$ mm). The scales in A and B are (per square) for time: 0.05 s; fiber length: 10 μm ; apparent sarcomere length: 7.3 μm ; intensity: 20% of the initial value. The velocity at the moving end was 129 $\mu\text{m}/\text{s}$, and the fiber was illuminated at a position equal to 62% of its length from the fixed end. Therefore, the translation through the center of the beam during one oscillation was expected to be $0.62 \times 129 \times 0.034 = 2.7$ μm . The apparent sarcomere length was 2.73 μm , as estimated from the position of the first order beam before stretch. In B, during the initial 100 ms there was overlap of the records of fiber length and striation spacing at high scattering. The laser beam was distorted by the scatterers, and this altered the overall change in apparent sarcomere length as discussed in the text. The fiber length was 3.04 mm, and the cross section was 67 $\mu\text{m} \times 72$ μm .

intensity was raised to $\approx 4\%$ of that on the diffraction order, and the amplitude of oscillation dramatically increased. The frequency of oscillation was unaffected by changes either in h or scattering. The oscillations were reduced substantially

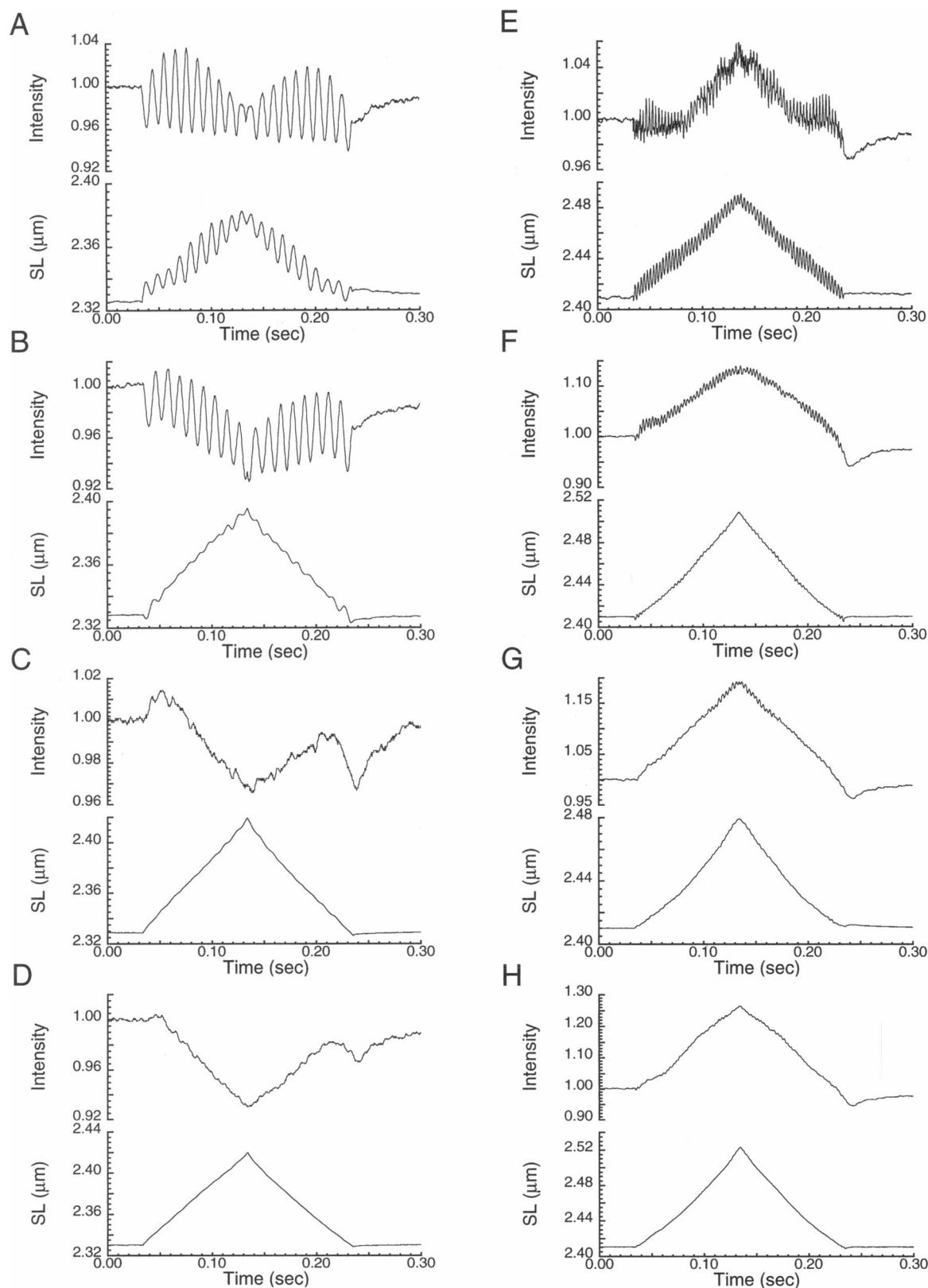
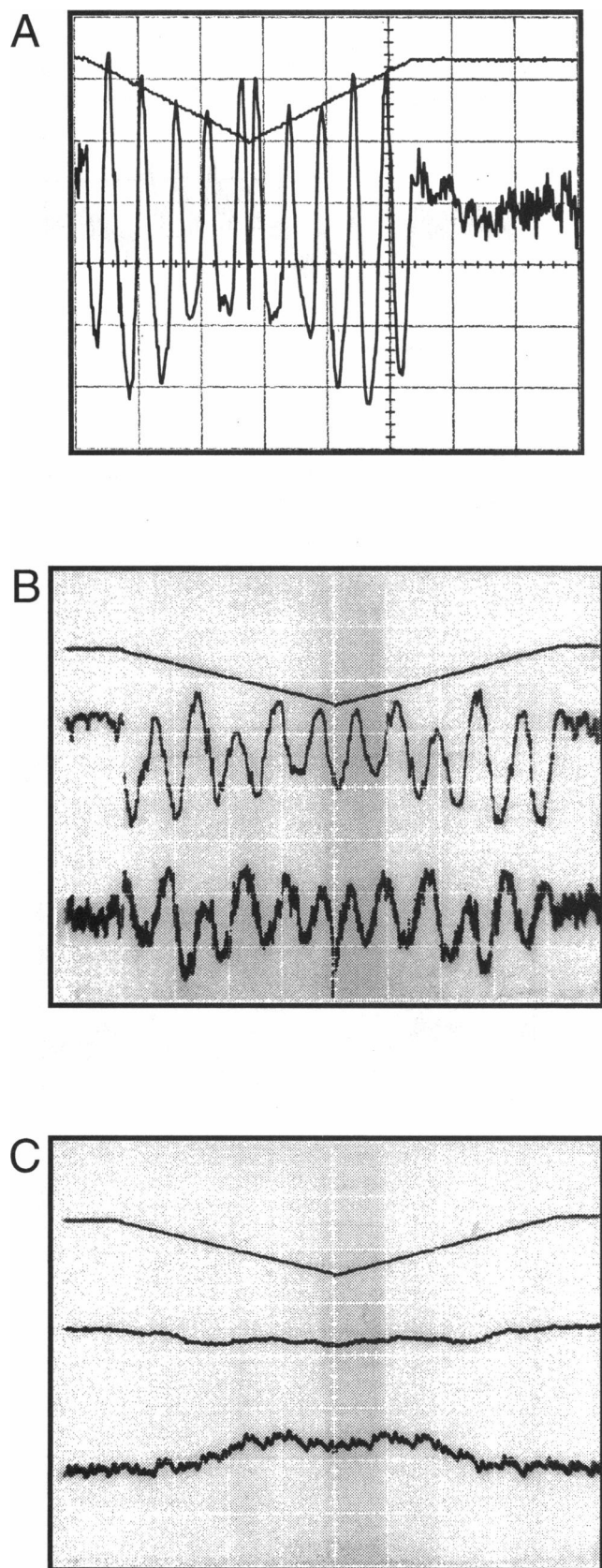


FIGURE 2 Stretch and release observed at two positions along a fiber and at various values of h in the presence of low and high scattering. Scattered light was produced by a glass filament. For each set of conditions in *A–H*, intensity (*top*) and sarcomere length signal (SL) (*bottom*) are shown. Intensity is expressed relative to the initial value in each record. *A–D* were taken with the beam positioned near the fixed end of the fiber, and *E–H* near the moving end. At each of the two positions, data are shown for h varied from a low value (fiber near the source of scattering) to a high value in the first three panels (*A–C* and *E–G*) at high scattering intensity. The fourth panel at each position (*D, H*) was recorded at high h and low scattering intensity. The values of h (mm) and intensity of scattered light (% diffracted) were respectively: (*A*) ≈ 0.2 and 4.8; (*B*) 0.6 and 4.8; (*C*) 1.8 and 5.6; (*D*) 1.8 and 0.38; (*E*) ≈ 0.2 and 4.6; (*F*) 1.6 and 5.5; (*G*) 2.5 and 5; (*H*) 2.5 and 0.42. The intensity of scattering is given relative to the diffraction intensity averaged across the order. The values would be reduced by about one-half if expressed relative to the intensity at the center of an order with a Gaussian intensity profile (see Materials and Methods).



by simultaneously increasing h and reducing scattering (Figs. 1 *B* and 2, *D* and *H*). If the peak-to-peak amplitude of the oscillatory component of centroid movement was comparable with the magnitude of steady change in an equal time, then the apparent sarcomere length record contained alternating periods of little change and change at about twice the true rate (Figs. 1 *A* and 2, *B* and *F*).

A disadvantage of using beads to generate scattered light was that the intensity profile of the laser beam was distorted and a significant portion of the incident light was no longer collimated. This had the effect of illuminating a larger portion of the fiber with a range of intensities and angles of incidence. In addition, for nonzero angles of incidence of the laser beam, new areas of the scattering material were illuminated when h was changed by vertical movement of the chamber containing the bathing solution. This further altered the distribution of angles and intensities of light incident on the fiber. As a result, overall changes in apparent striation spacing were often altered by the presence of scattered light and changes in h (Fig. 1). To reduce these effects, a scatterer much smaller than the laser beam was used. Scattered light was produced by a glass filament (35- μm diameter) lying on the bottom of the chamber perpendicular to the fiber axis, which refracted a fraction of the beam into a bright, narrow line along the meridian of the pattern (see Fig. 7 *D*). In this case, much of the laser beam was not scattered and the diffraction orders were much less distorted. Light scattered from the glass filament resulted in oscillations with the same properties as those observed with other types of scatterers, but the overall change in apparent sarcomere length was less affected (Fig. 2).

The amplitude of oscillation depended on the part of the diffraction pattern that illuminated the photodetector. This was controlled by a slit of adjustable width in front of the photodiode. When the slit was ~ 5 times the width of the diffraction order, the oscillation in apparent spacing increased significantly over that observed when the slit was approximately equal to the diffraction order linewidth (Fig. 4, *A* and *B*). If a slit narrower than the diffraction line was positioned on and off the order, the centroid oscillation actually could be larger off the order, whereas the intensity oscillation was always larger on the order (Fig. 4, *C* and *D*).

FIGURE 3 Translation of fiber and grating through the beam. (A) Oscillation in first-order centroid resulting from axial translation of an entire fiber through the laser beam. The upper trace shows fiber displacement (10 $\mu\text{m}/\text{square}$) and the lower trace oscillation in apparent spacing (2.7 nm/square). The timebase was 0.05 s/square . The amount of translation per oscillation, averaged over the first four full cycles, was 2.60 μm . The sarcomere length estimated in the absence of added scatter was 2.63 μm . The fiber-scatterer separation (h) was ~ 0.2 mm. Oscillations resulting from translation of a grating through the beam are shown at low h (0.25 mm) in *B* and high h (3.65 mm) in *C*. The grating was translated by 10 μm , representing 5.24 periods. In *B* and *C*, the traces show (from top to bottom) translation (10 $\mu\text{m}/\text{square}$), apparent spacing (1.3 nm), and intensity (1.6% initial value) versus time (0.05 s/square).

Evidence presented below shows that these effects can be explained by interference fringes present on and off the diffraction order.

Having traced the phenomenon to the presence of scattered light, we developed a theoretical description that shows that oscillations of this kind, and of the observed order of magnitude, are expected to result from interference of scattered light with the light diffracted by the fiber. The mechanism is quantitated in the Appendix and may be described qualitatively as follows:

- 1) When the fiber is translated parallel to its axis, the phase of the first-order diffracted beam (relative to that of the incident light) is shifted by an amount proportional to the displacement of the fiber, the amount of the phase shift being exactly 1 cycle per sarcomere length of displacement.
- 2) Interference between the scattered light and the light in the diffracted beam causes variations of intensity within the diffracted beam, so that its centroid is displaced from where it would have been if there had been no scattered light, i.e., the presence of the scattered light causes an error in the apparent diffraction angle.
- 3) This error will vary with the relative phase of the scattered and diffracted light, going through one cycle when the phase difference alters by one cycle, i.e., according to (1)

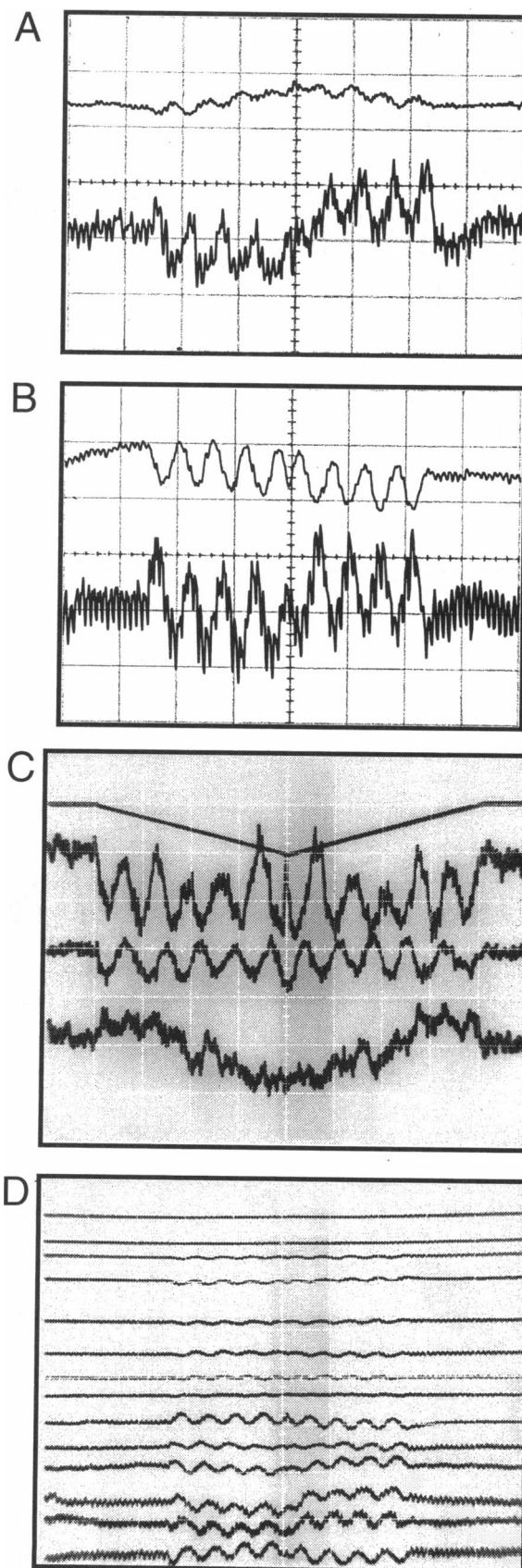


FIGURE 4 Oscillations on and off the first order. (A, B) Example of the effect of masking the diffraction pattern so that light away from the first order did not contribute to the photodiode signal. Translation of a relaxed fiber by $10\ \mu\text{m}$ began at 0.3 s into the record and was reversed 0.5 s later. A masks in near to the first order, B masks out to about 5 times the width of the order. In A and B, the top trace is apparent spacing and bottom trace intensity. The scales are $5\ \text{nm/square}$ in both panels for spacing, 0.7 and 0.5% for intensity in A and B, respectively. The horizontal scale is 0.2 s/square, equivalent to $4\ \mu\text{m}$ translation. The translation over the first three full oscillations in the spacing signal of B was $7.2\ \mu\text{m}$, giving $2.4\ \mu\text{m/oscillation}$. The estimated sarcomere length was $2.42\ \mu\text{m}$. The intensity signal was AC-coupled, and there was a slow change during translation, such that a small offset resulted halfway through the record when the direction of translation was reversed. (C) A small slit ($0.1\ \text{mm}$) was placed at various positions in front of the photodiode on and off the first order ($\approx 1\ \text{mm}$ wide) produced by a diffraction grating. The photodiode was positioned 329 mm from the fiber. The top trace represents movement of the grating through the beam, and the lower three traces show resulting oscillations in the centroid signal with the slit at (top to bottom) 8, 0, and $-4\ \text{mm}$ along the meridian from the brightest part of the first order (positive on the zero-order side). Scale is $10\ \mu\text{m/square}$ for translation and is $0.58\ \text{nm/square}$ for apparent spacing with the slit positioned on the order, $0.73\ \text{nm}$ off the order. Time is 0.2 s/square. The translation during each oscillation averaged over the records from the 8 and 0 mm positions was $1.85 \pm 0.8\ \mu\text{m}$ (mean \pm SEM, $n = 16$); the grating period was $1.90\ \mu\text{m}$. (D) A series of intensity records showing oscillations resulting from translation of a fiber with a $0.5\ \text{mm}$ slit positioned along the meridian at $0.5\ \text{mm}$ intervals on and off the first order. The photodiode was positioned 810 mm from the fiber. The average intensity, expressed relative to the value obtained with the slit over the brightest part of the order, was (starting at the bottom record) 0.86, 1.00, 0.89, 0.43, 0.34, 0.17, 0.13, 0.12, 0.098, 0.077, 0.089, 0.062, 0.048, and 0.047. The intensity/square is 8.5% of the maximum (as measured at the slit position corresponding to the 2nd record from the bottom). An offset at the center of some records is present for the reason given in A.

above, when the fiber has been shifted longitudinally by one sarcomere length.

Fringes arising from the presence of scattered light

As mentioned in the preceding section, we observed fluctuations of intensity and of centroid position when the muscle fiber was displaced axially, even when the slit in front of the photodiode did not admit any of the diffraction orders. This suggested that interference fringes were present even away from the diffraction orders. An attempt was made to track the movement of such fringes by measuring the change in phase of the intensity fluctuations when the position of the slit, along the meridian of the pattern, was changed. However, because drift of only a fraction of a micron in the servomotor position caused significant phase shifts, and positioning of the slit was slower than such drift, the experiments were not satisfactory. An alternative approach was to view the pattern directly, and records were made using a video camera. Scattered light in the form of a narrow line along the meridian of the pattern was produced by a glass filament (Fig. 7 *D*). The glass filament could be moved out of the beam easily, allowing the diffraction pattern to be viewed in the absence of added scatter (Fig. 7 *C*). In these experiments, the diffraction order was not focused to a spot.

When a muscle fiber was positioned in the beam, the light refracted from the glass filament broadened in the equatorial direction because of additional refraction of a part of the light through the fiber. The light scattered by the filament produced a series of fringes along the meridian (Figs. 5–7). These fringes were visible both near the first order (Fig. 5) and well away from the order (Fig. 6), and they had similar spacing in both cases. Fringes were present whether the filament was placed below or above the fiber. A difficulty with this experiment lay in distinguishing the fringes from fine structure on the diffraction orders and speckle off the orders,

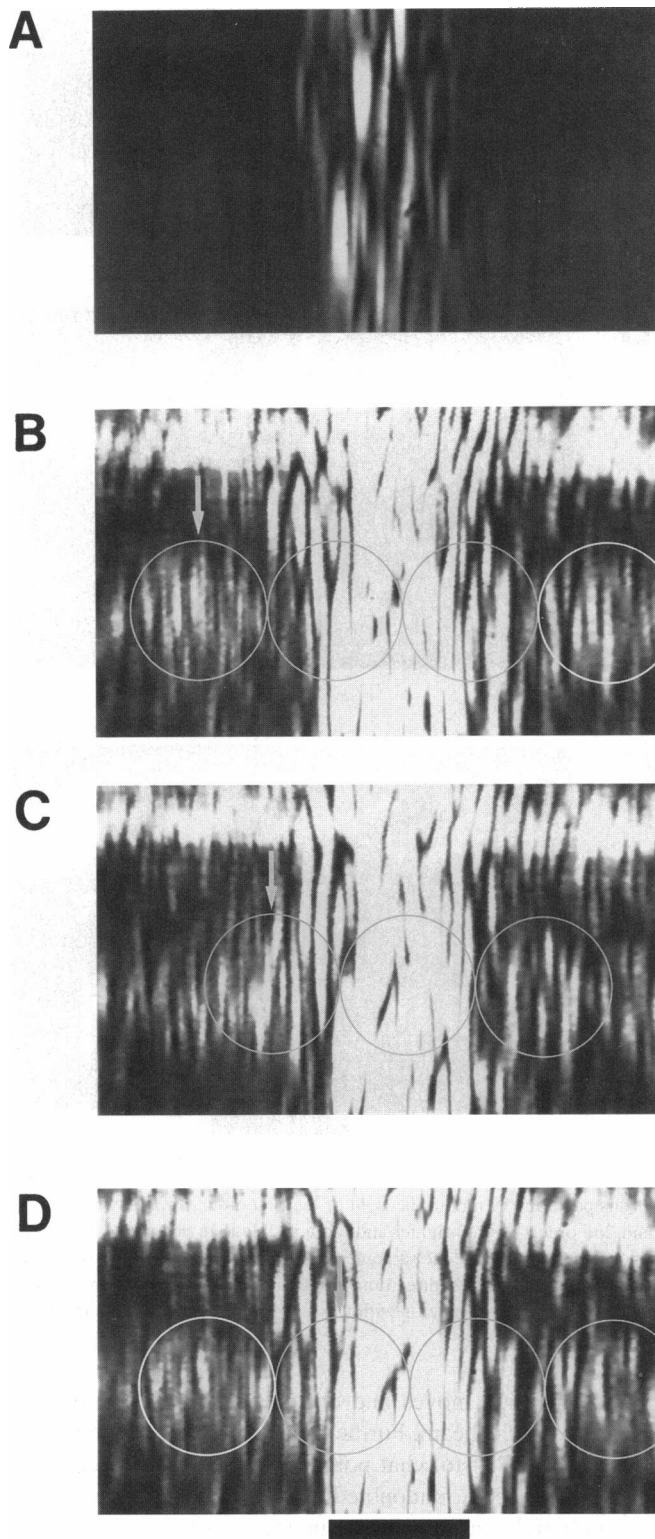


FIGURE 5 Interference fringes on the first order. (A) Part of the right first-order line at the meridian is shown. Light scattered from a glass filament (see Materials and Methods and Fig. 7 *D*) is present. The vertical stripes are fine structures in the order. (B) As in A, but with intensity of illumination increased to make the background more visible; the diffraction order saturated the camera in this case. In addition to a complex pattern of spots and fine structures, a periodic pattern of fringes is observed in the background and four of these are circled, the inner two of which lie partially on the order. In C and D, the fiber was translated to the right of its position in (B) by 0.5 and 1 sarcomere length ($2.37 \mu\text{m}$), respectively. The right-hand fringe in B moves out of the field of view to the right, and the left-hand fringe in D moves in from the left during the translation. An arrow points to the same fringe at the three positions shown in B–D. The fringe spacing was about 2.0 mm, consistent with a value of 2.06 mm predicted by the theory given in the Appendix. The brightest part of the first fringe in B was about 8% of the brightest part of the diffraction order, which is of the order (4%) expected from the theory described in the Appendix. The laser beam was incident on the fiber from the right at an angle of 7.9° . At this angle of incidence and $s = 2.37 \mu\text{m}$, $\theta = 7.4^\circ$ (with respect to a line drawn normal to the fiber). The video camera was 174 mm from the fiber (bar = 2 mm at the camera).

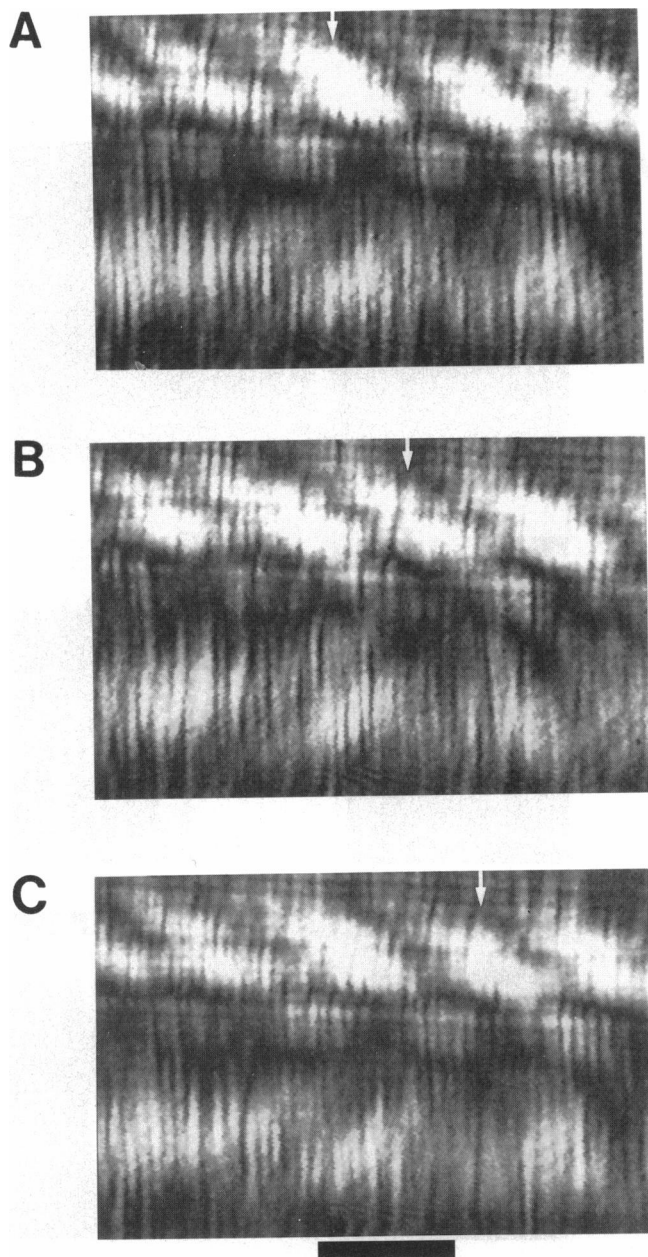


FIGURE 6 Fringes off the diffraction order. As in Fig. 5, but the fringes at this position (19 mm to the right of the first order, 36% between the 1st and 2nd orders) were brighter and more visible than nearer the order. The fiber was translated by one sarcomere length from A to C. The arrows point to the same fringe at the three time points shown. Note that the intensity of different fringes at a given position is nearly constant (bar = 2 mm).

much of which moves and changes form when a fiber is displaced in the beam. Furthermore, the shape of the fringes varied according to what point on the fiber was positioned in the laser beam, undoubtedly due in part to refraction of scattered light through the irregular cross section of the fiber. However, when the fiber was translated the fringes moved smoothly in the same direction as the fiber, and this property aided in revealing them. The velocity of fringe movement was directly proportional to the velocity of fiber translation, such that the time required for the fringe pattern to shift by

one period was equal to that for the fiber to be displaced by one sarcomere length (Figs. 5 and 6). The spacing between the fringes decreased as the separation between fiber and scatterer increased (Fig. 7, A and B). The change in fringe spacing did not alter the relationship between fringe movement and fiber displacement. This had the effect of slowing the movement of fringes at lower fringe spacing, such that

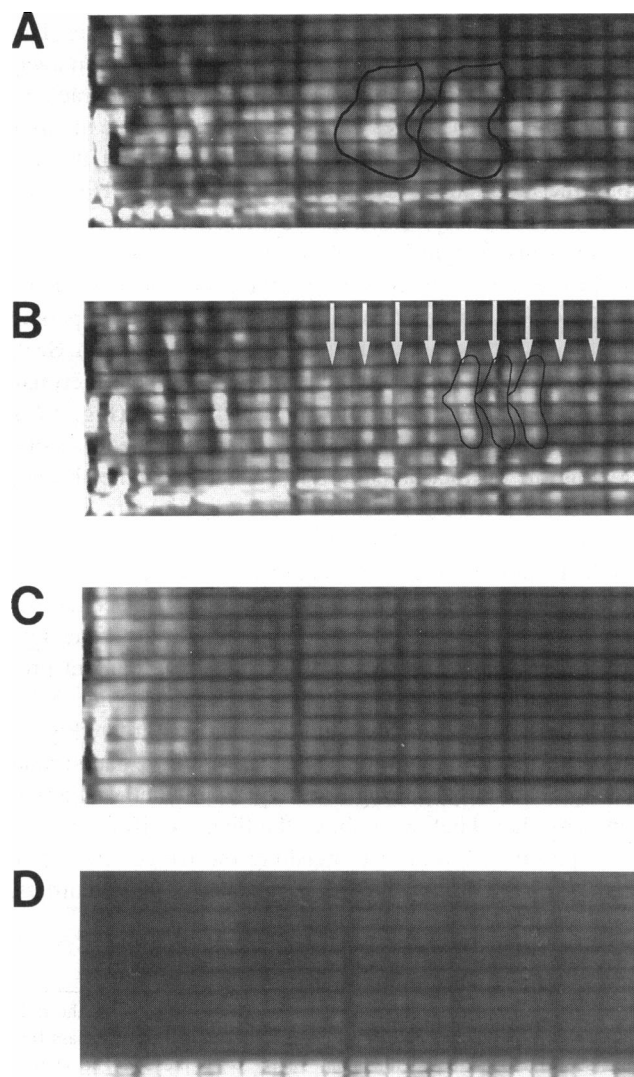


FIGURE 7 Variation in fringe spacing with fiber-scatterer separation. A millimeter grid was illuminated by the diffraction pattern. A set of fringes at $h \approx 0.15$ mm is shown in A, and the two brightest fringes are outlined. The edge of the right first order is to the extreme left of the figure. In B, h was increased by 0.25 mm to $h \approx 0.4$ mm, and three of the fringes are outlined. The arrows indicate equivalent positions on nine of the fringes which, as in A, were distinguished from the background by movement during fiber translation. The spacing between the fringes decreased by a factor of about 2.7 between A and B, and this factor is nearly equal to the value expected theoretically (spacing inversely proportional to h). The same area of the pattern is shown in C with the fiber alone (no added scatterer). The data in D was acquired with the glass filament scatterer alone (fiber out of the beam) from the same area, but shifted slightly left with respect to A–C to show the scatter at the location of the first order. The relationship between brightness (greylevel) in the photographs to intensity in the video data is the same in A–D. The angle of incidence was 7.9° , the distance between the fiber and screen was 197 mm at the 1st order, $\theta = 6.87^\circ$ at $s = 2.46 \mu\text{m}$.

the intensity at a given point in the diffraction pattern always underwent one cycle of oscillation for each sarcomere length displacement. This intensity oscillation at a given point was observed even when h was large (≥ 0.5 mm) and fringe spacing had decreased to the extent that fringes became indistinguishable from background speckle. Even if the only scatterer was that from the glass bottom of the chamber (Fig. 7 C), in which case fiber displacement caused no observable centroid oscillation, the remaining spots and fine structure still contained a component of intensity oscillation at the same frequency. It was observed further that fringe intensity was not constant off the order but usually exhibited a maximum over a narrow range of diffraction angles. For example, Fig. 6 shows fringes far off the order that were actually brighter than those of Fig. 5 near the order. The scatter however did not change significantly over the same range of angles (Fig. 7 D). The intensity of fringes passing through such regions during fiber displacement always rose and then fell (Fig. 6), indicating that increased intensity was not associated with any given fringe. The intensity of the second order was also observed to oscillate during fiber translation, but with a strong component at twice the frequency of the first order (Fig. 8). This is expected on the theory described below because the phase of the diffracted light at the second order shifts through two cycles when the fiber is translated by one sarcomere length.

Theory accounting for oscillations

A quantitative theory describing interference between diffracted and scattered light was developed to account for our observations. The derivation is given in the Appendix, and the result is given in Eq. 1. Here we compare predictions of the theory to experiment and also discuss additional assumptions required to explain some of our observations.

In the simple case of a diffracted beam of square intensity profile in the presence of light scattered by an object at a

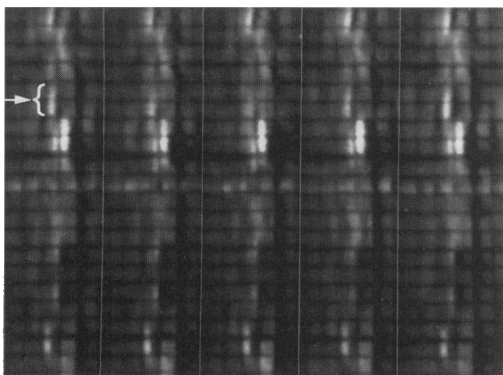


FIGURE 8 Intensity oscillation on the second order. A sequence of images showing the 2nd order during translation of the same fiber as in Fig. 7. Movement of $0.31 \mu\text{m}$ occurred between each image, giving a total of $1.23 \mu\text{m}$, or one-half sarcomere length, during this series. Each fine structure exhibited some intensity oscillation, going through one cycle during translation of the fiber by one-half sarcomere length. The arrow points to a region showing a relatively large intensity oscillation.

distance h above or below the fiber, the maximum deviation of the centroid from its position in the absence of scattering is

$$d\bar{x} = \frac{2\epsilon}{\alpha^2 w} \left[\sin\left(\frac{\alpha w}{2}\right) - \frac{\alpha w}{2} \cos\left(\frac{\alpha w}{2}\right) \right], \quad (1)$$

where w = width of diffracted beam at the detector, $\epsilon = 2ab/(a^2 + b^2)$, a = amplitude of diffracted light and b = amplitude of scattered light, $\alpha = 2\pi nh/rs$, and r = distance between scatterer and detector, s = sarcomere length, and $n = 1, 2 \dots$ for first, second, etc. order diffraction.

Equation 1 is oversimplified in assuming that diffraction intensity and, therefore, intensity of the interference fringes are zero off a diffracted beam of width w . Intensity between diffraction orders could arise from light scattered in a random manner by structures other than the striations in the fiber (e.g., nuclei, mitochondria, fat droplets, etc.), and there also could be a contribution from random variation in striation spacing. The fringes seen between the diffraction orders would then be due to interference between this scattered light and light due to scatterers above or below the fiber. Because these scatterers move with the fiber, the argument used in the first paragraph of the Appendix applies, and light scattered by them near the n th diffracted beam will undergo a phase shift that cycles through n periods when the fiber is displaced through a distance equal to the striation spacing, and the fringe pattern will shift by one fringe at the first order, two fringes at the second order, and so on. However, within the accuracy of measurement (a few percent of the fringe spacing), the entire fringe pattern always moved by one period for displacement of the fiber by one sarcomere length. For example, the fringes shown in Fig. 6 were at a diffraction angle about one-third of the way between the first and second orders and, yet, they clearly moved by one period for movement of one sarcomere length. Furthermore, fringe spacing should decrease with increasing diffraction angle so that the spacing at the second order would be one-half the value at the first order. However, this prediction is inconsistent with the observation that the fringe spacing was that expected for the first order, even well away from the order (Figs. 6 and 7). An alternative explanation is that a portion of the scattered light incident on the fiber is itself diffracted by the striations. Because scattered light illuminates the fiber over a continuous range of angles of incidence, this secondary diffraction would not produce discrete orders but, rather, the light corresponding to a given order would be spread out over a range of θ . The fringe pattern at a given θ would be dominated by light of the brightest orders produced by secondary diffraction. In most of our experiments, the first-order diffraction angle was near the Bragg angle, and it is expected that most of the pattern near the first order arising from secondary diffraction would correspond to first-order light. The spacing and movements of the fringe pattern were characteristic of the first order and are consistent with this explanation. The relationship of the fringe intensity to the Bragg angle is considered at the end of the Discussion. An estimate of the intensity of secondary diffraction is given in the Appendix, and a comparison

between fringe intensity measured off the order and that calculated from the theory is made in the legend to Fig. 5.

We also note that interference between light diffracted by the striations and light scattered randomly by the fiber does not account for the fringe pattern we observe. If this were the case, the phase shift between the two sources would not change as a fiber is translated and, hence, the movement of fringes would be equal to fiber displacement, which is clearly inconsistent with experiment.

Equation 1 also can be made more realistic by assigning a Gaussian intensity profile to the diffracted beam and this is done in the Appendix (Eq. A7). A description is also given in the Appendix of a modification to the term for diffraction amplitude (a) to account for the contribution of secondary diffraction to light between the orders. The results of these calculations are shown graphically in Fig. 9. Interference between the scattered and diffracted beams results in periodic intensity fringes in the pattern (Fig. 9, *A* and *B*). As a fiber is translated, the phase of these fringes is displaced in the same direction as the fiber, going through one cycle for fiber translation by one sarcomere length (Fig. 9 *C*). This causes the apparent centroid to oscillate with an amplitude that is well approximated by Eq. 1. Intensity integrated across the detector similarly oscillates, but shifted by one-quarter cycle from the centroid oscillation (Fig. 9 *D*). The calculated separation of the interference fringes decreases with an increase in fiber-scatterer separation (Fig. 9, *A* and *B*), resulting in reduced centroid oscillation (Fig. 9 *E*). Decreasing h is also expected to reduce the oscillation in intensity (Fig. 9 *F*). The theoretical curves shown in Fig. 9, *D* and *E* are not strongly dependent on the shape of the intensity profile, although a square profile reduces the calculated intensity oscillation at low h (<0.6 mm in Fig. 9 *F*). The minima and maxima in Fig. 9, *E* and *F* result from cutoff effects due to integrating intensity over a finite interval. These theoretical results are generally consistent with experiment.

As observed in Fig. 5 and calculated in Fig. 9 *A–C*, fringe visibility (intensity relative to background) is

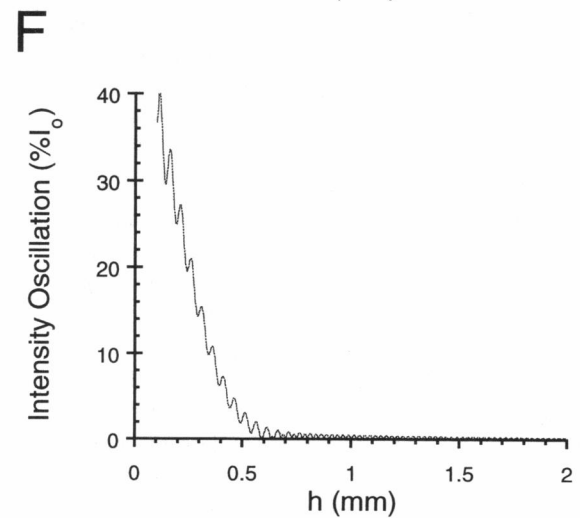
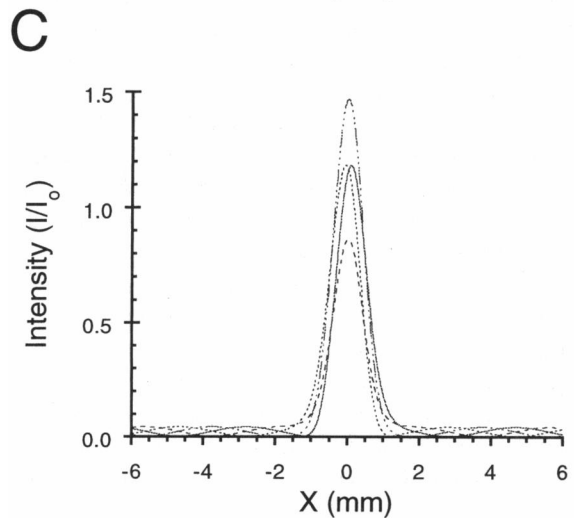
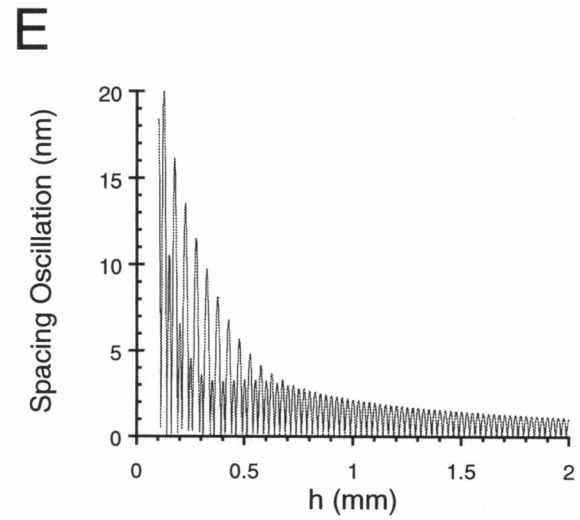
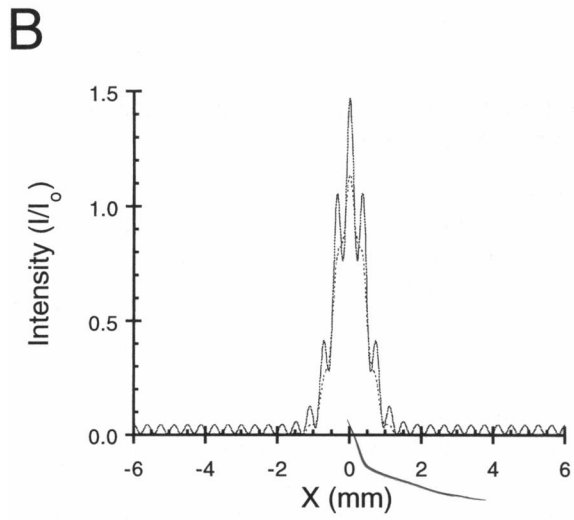
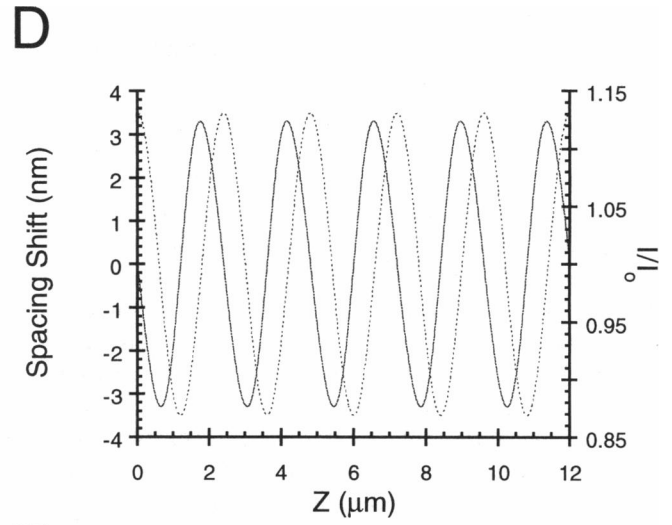
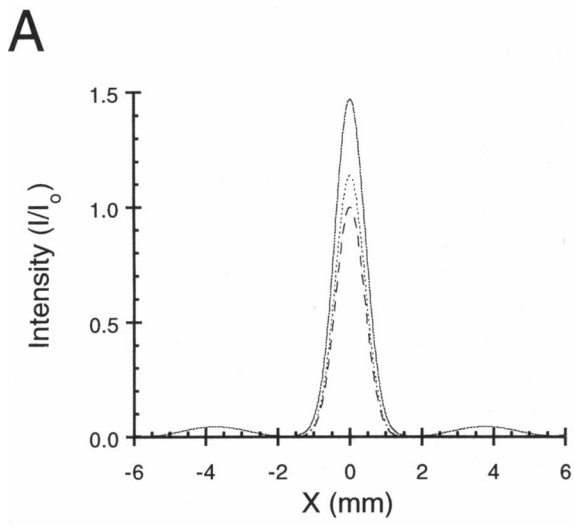
larger off the diffraction order than on and is the result of the intensities of scattered and diffracted light being more nearly equal. This accounts for the observation that centroid oscillation can increase when the signal includes contributions from off-order light (Fig. 4 *A–C*), as is frequently required to allow for movements of the order corresponding to changes in sarcomere length. However, the absolute intensity of the fringes is expected to be higher on the order, accounting for greater intensity oscillation there (Fig. 4 *D*).

DISCUSSION

Identification and elimination of oscillation artifact

We have identified interference between scattered and diffracted light as a source of oscillations in apparent striation spacing estimated by laser diffraction. The oscillations appear when the illuminated portion of a fiber is translated through the laser beam, as occurs during stretch or release. As first reported by Altringham et al. (1984), the oscillations in centroid go through one cycle for each sarcomere length of displacement. Oscillations in intensity occur at the same frequency. This relationship held over all the translation speeds used, producing oscillation frequencies of a few Hz to hundreds of Hz. The presence of the oscillations was not dependent on sarcomere length or state of activation. The superposition of such oscillations onto a steady change in striation spacing can give the appearance of “pauses” and “steps” in the estimate of sarcomere length (Pollack et al., 1977). Because the oscillation frequency depends on the position of a fiber illuminated during a length change, changes in measured sarcomere length appearing most like pauses and steps can result from a relatively small amplitude, high frequency oscillation near the moving end, or a relatively large amplitude, low frequency oscillation near the fixed end. There obviously would be no justification for assigning special significance to those “pauses” during which sarcomere length appears to be nearly constant.

FIGURE 9 Predictions of theory. (*A*) Plot of total intensity versus meridional position at the first order in the absence and presence of scattered light. The intensity distribution was modeled to be Gaussian ($\sigma = 0.2$ mm). Total intensity is expressed relative to the value at the center of the order in the absence of scattering ($I_0 = a^2$). Calculations were done for scattered light at three intensities: $b^2/a^2 = 0$ (— — —), 0.0025 (- - -), and 0.025 (— — —). The variables used in the calculations were (see Appendix): distance from fiber to position of photodetector or screen (r) = 312 mm; fiber-scatterer separation (h) = 0.2 mm; grating spacing (s) = 2.4 μ m. The fringes shown away from the diffraction order result from additional diffracted light arising from scattered light incident on the diffractor. The proportion of scattered light that is diffracted (δ) is assumed to be 0.2 (see Appendix). The axial position of the fiber and, hence, the phase of the interference fringes, was chosen such that the fringe pattern is centered on the first order ($z = 0$). (*B*) As in *A*, except h has been increased to 2 mm and no example is shown for zero scattered light. The fringes now contribute to fine structure on the order. (*C*) As in *A*, but only for $b^2 = 0.025$. The fiber is translated axially (z -varied) and intensity versus x calculated for $z = 0$ (total intensity at maximum during oscillation), $0.25s$ (centroid at maximum), $0.5s$ (intensity minimum), and $0.75s$ (centroid minimum), where s = sarcomere length. The peak traces out an ellipse in which intensity and centroid are 90° out of phase and oscillate once during translation by $z = s$. (*D*) Oscillations in striation spacing (— — —) and intensity (- - -) as the fiber is translated through five periods ($\Delta z = 5s$). The spacing calculated from the centroid position and total intensity are plotted as a function of z . The spacing oscillates by 6.52 nm (peak-to-peak), which corresponds to an oscillation in the position of the centroid by 0.226 mm at the detector as shown in *C*. The two traces are one-quarter period out of phase. The quantities used in the calculations are as in *C*. The intensity and position of the centroid were calculated by numerically integrating around the first order over 75σ , which is equivalent to an unmasked pattern in the current experiments. If superposed on a ramp of appropriate slope to produce a staircase, the “steps” in spacing would be twice this value, or about 13 nm. (*E*) Spacing oscillation as a function of fiber-scatterer separation (h). Peak-to-peak values are shown. (*F*) Intensity oscillation versus h . For calculations in *E* and *F*, the variables were set to the values used in *C* and *D*, which were approximately those in the experiments of Fig. 2 *A–C* and *E–G*, in which oscillations were present on ramp stretch and release of a relaxed fiber.



In the presence of scattered light of less than 1% of the diffraction intensity, we observed oscillations equivalent to 2–10 nm in sarcomere length, which would correspond to “steps” of 4–20 nm when superposed on a ramp length change (Figs. 1 and 2), similar to those reported by Pollack and colleagues (e.g., Granzier and Pollack, 1985). The oscillation amplitude was reduced to less than the noise level of our signals (≈ 0.5 Å sarcomere length over 100 Hz), by either reducing scattered light or moving the fiber a few millimeters away from the source of scattering. The amount of scattered light produced by, for example, an air/glass and glass/solution boundary at the bottom of the chamber was not sufficient to produce oscillations in the centroid of the diffraction order, even for a fiber within a few tenths of a millimeter of the (clean) glass. Under these conditions in a separate series of experiments, several hundred laser diffraction records have been obtained during stretch and release of active and relaxed single fibers without oscillations of the type described here. Therefore, the reliability of laser diffraction in estimating mean sarcomere length need not be compromised by this source of artifact.

Our results do demonstrate the importance of keeping the illuminated area of the experimental chamber clean to minimize scattering. The effect of interference fringes also applies to static estimates of sarcomere length made on non-moving fibers, although the error is small relative to the length of an entire sarcomere (generally <1%). The error resulting from oscillations also could be reduced by integrating the diffraction signal (onto film or an electronic camera) while scanning a laser beam along a fiber over a distance of a few sarcomere lengths.

The observations reported here may account for reports of oscillations in sarcomere length from early studies using laser diffraction (Goldspink et al., 1970). Oscillations were reported to occur during isometric tetani of chick muscle, and it would be surprising if some movement of striations had not occurred during contraction of the whole muscle. It is worth noting that the muscle was positioned very near glass plates through which the laser beam passed, thus minimizing the distance between a possible source of scatter and the muscle. Such oscillations, however, were not observed in subsequent laser diffraction studies on single fibers (Cleworth and Edman, 1972; Kawai and Kuntz, 1973).

Visibility of the interference fringes is expected to be maximum when the intensities of the scattered and diffracted light are equal. This relationship would explain the higher visibility of fringes off the diffraction order, where the intensity of scattering is a much higher proportion of the total than on the order. These off-order fringes can account for the observation that the amplitude of oscillation increased as a slit placed in front of the photodetector was widened. The proportion of scattered light at the diffraction order increases when diffraction intensity is low, as can occur, for example, when the angle of incidence is far from the Bragg angle or if the striations are disordered. Low diffraction intensity would increase the amplitude of oscillation in disordered preparations and could explain the observation of Altring-

ham et al. (1984) of larger oscillations in “areas of the fiber giving less than optimal signal quality”.

Although we have characterized the oscillations only in the far-field diffraction pattern, periodic fringes could well be present in the near field. Indeed, fringes were apparent even within a few millimeters of the fiber. When imaging striations using laser illumination, the fringe pattern could superimpose on the striation image due to the very large depth of field. As in the far field, the fringe pattern would be displaced in the same direction as striations during length changes. Unless the fringe and striation periodicities were identical, an oscillatory shift in apparent striation position and average spacing would result. Consideration should be given to possible effects of interference fringes in the presence of scattering when imaging striations using collimated laser light (Pollack et al., 1986; see also discussion of oscillations in both signals given by Huxley, 1986).

Additional sources of artifactual fluctuation and methods of correction

It should be emphasized that there are other sources of artifact, both optical and instrumental, that can produce erratic fluctuations in apparent sarcomere length that appear as a sudden acceleration or deceleration during an otherwise steady length change. Errors in sampling the striations can result from Bragg reflections, and evidence for this has been provided by several groups (Rüdel and Zite-Ferenczy, 1979b; Altringham et al., 1984; Lieber et al., 1984). It was also shown by Goldman and Simmons (1984) that sampling striations over a range of incident angles could eliminate irregular fluctuations in apparent sarcomere length that sometimes occurred during shortening of skinned frog fibers. However, changes in striation tilt and spacing that alter the intensity of Bragg reflections are unlikely to cause regular fluctuations, especially at a frequency directly related to the movement of striations through the beam. The oscillations observed with a plane grating further show that Bragg effects are not required to explain regular cascades of steps during steady changes in striation spacing.

If a microscope image is formed with laser light, as was done by Delay et al. (1981), Abbe's theory of the formation of a microscope image shows that the apparent spacing in the image (e.g., of striations) is inversely proportional to the sine of the angle through which the light entering the microscope objective is diffracted by the specimen. Hence, shifts in the directions of the diffracted beams caused in the way described in the present paper will cause corresponding changes in the spacing of the striations seen in the microscope image, as was pointed out by Huxley (1986).

“Pauses” were also seen by Jacobson et al. (1983) using their “phase-locked loop” method, which is not susceptible to the errors discussed here because a white light source was used. Altringham et al. (1984) showed that even in this case the fluctuations occurred once per sarcomere passing the point of observation, showing that they must be of instrumental origin; an explanation based

on a feature of the electronic circuits was suggested by Huxley (1984).

In addition to the methods described here for eliminating the oscillations, illumination by light of reduced coherence would decrease the visibility of interference fringes. The visibility of the diffraction orders would also decrease, but generally to a lesser extent, because the spatial separation between the fiber and a source of scattering is greater than between striations giving rise to the diffraction orders. Illumination with less coherent light would also have the advantage of reducing part of the fine structure on the diffraction order resulting from interference between spatially separated domains of striations (Brenner, 1985; Sundell et al., 1986). Goldman (1987) showed that spurious steps during changes in sarcomere length could be eliminated in this way. Goldman also observed cascades of steps and pauses during shortening of partially activated frog skinned fibers and eliminated these using a white light diffraction system. He pointed out that this result may have been due to multiple wavelengths sampling over a range of striation tilts or, alternatively, the reduced coherence of white light may have been responsible. As discussed in the Appendix, the intensity of the fringes we describe here is expected to be reduced greatly using white light diffraction and this effect may also have contributed to his results. Goldman's result using laser light of reduced coherence and the observations reported here do argue for phase-randomizing the laser illumination, as has been done in light microscopy (Hard et al., 1977; Ellis, 1979).

Limitations to theory

The theory developed in the Appendix shows that interference between diffracted and scattered light accounts satisfactorily for several properties of the oscillations. These include the dependence of frequency on speed of striation displacement, the dependence of amplitude on intensity of scattered light and on fiber-scatterer separation, and the presence of interference fringes in the diffraction pattern that move along the meridian when the fiber is translated axially. Although there is fair agreement between the observed and theoretical values for the oscillation amplitudes, exact agreement is not to be expected for several reasons. The theory does not take into account factors such as irregularities in the striations, a range of values of h due to fiber thickness, fine structure on the order, or speckle off the orders. For example, the fringes observed at various positions of the beam along and across a fiber are highly variable in form, probably due in part to refraction through the fiber cross section, which is variable in shape. It is not surprising then that the oscillations in centroid and intensity vary in amplitude as a fiber is displaced. As the separation of the fiber and scatterer was increased, the spacing of the interference fringes decreased (Fig. 7), and it became difficult to distinguish them from the speckle and fine structure. However, the presence of the phenomenon still was revealed by intensity oscillation of individual speckles, which went through one cycle per sarcomere length displacement.

Uses of the interference pattern

An advantage of the phenomenon that is readily apparent is the direct relationship of the oscillations to displacement of striations through the beam. This has already been exploited in the "striation follower" device of Huxley et al. (1981a, b) in which one diffracted beam is recombined with the zero-order beam rather than undergoing interference with scattered light. To convert number of striations to fiber displacement, it is necessary to know the striation spacing; in the "striation follower," this has to be determined independently, either by microscopic observation or by displacing the fiber through a known distance to calibrate the signal from the interference pattern. The striation spacing, however, can be estimated simultaneously by measurement of the diffraction angle.

Another potential advantage of the fringes suggests itself from the observation that the first-order fringe intensity regularly exhibited a maximum near, but frequently not on, the first order itself. The position of this maximum changed little during fiber translation by many sarcomere lengths, and the intensity of individual fringes rose and fell as they moved past. On the other hand, the intensity of scattering was essentially constant over the same range of diffraction angles. As discussed in Results and the Appendix, the off-order fringes are thought to arise from scattered light incident on the fiber over a range of angles and, hence, diffracted over a continuous range. As such, the intensity of this off-order diffracted light should vary along the meridian, depending on its angle of diffraction relative to the Bragg angle. The data of Fig. 7 A provide an example. The diffraction angle at which fringe intensity was maximum was $\sim 11.6^\circ$ (centered on the two outlined fringes). The sarcomere length was $2.46 \mu\text{m}$, so the Bragg angle for striations normal to the fiber was 7.4° . The difference between the two numbers can be explained by a striation tilt of $\sim 11.6 - 7.4 \approx 4^\circ$, which is well within the range of tilts generally observed in striated muscle and also reported from light diffraction studies (Rüdel and Zite-Ferenczy, 1979a; Baskin et al., 1981; Gilliar et al., 1984; Burton and Baskin, 1986). Thus, variation in fringe intensity with diffraction angle in principle could provide the same information about Bragg planes as obtained from the dependence of first-order intensity on angle of incidence ("omega scan," Rüdel and Zite-Ferenczy, 1979a). Both types of measurement on the same preparation would be required to test this hypothesis.

The experiments were carried out in the laboratory of Professor R. M. Simmons. The authors thank Mr. P. Stoneham for machining the diffractometer. We are also grateful to Dr. Lincoln Ford for helpful suggestions on a draft of this manuscript. Support for K. Burton was provided by the Medical Research Council (U.K.) during these experiments. K. Burton is grateful to the Center for Light Microscope Imaging and Biotechnology for facilities used to prepare the video figures and to Professor R. J. Baskin for the use of his laboratory to produce the left panel of the cover figure.

APPENDIX

Equations were derived to describe interference between diffracted and scattered light as shown in Fig. 10. For the incident beam normal to a diffractor

(e.g., a fiber or grating), the diffraction angle θ (measured in air) is determined by the spacing s and wavelength λ (also the value in air) through the equation $\sin \theta = n\lambda/s$, where n is the order number (1, 2, 3 ...), provided that refraction when the ray leaves the medium surrounding the fiber takes place at a surface perpendicular to the incident beam. By the sine rule, the angle between the diffracted and scattered beams (ϕ) is given by $\sin \phi = (h/r)\sin \theta$, where h is the separation between scatterer and diffractor and r is the distance to the photodetector. Imagine the diffractor initially at a position such that the diffracted and scattered beams are exactly in phase at the center of the n th order diffracted beam on the detector. The reduction of path length for the diffracted ray when the diffractor is displaced by a distance z to the right is $z \sin \theta$; because $\sin \theta = n\lambda/s$, the resulting phase shift, $2\pi(z/\lambda)\sin \theta$, is equal to $2\pi n z/s$ (diffracted beam advanced). The additional phase difference at a distance x from the center of the diffraction order is $\sim 2\pi(x \sin \phi)/\lambda = 2\pi n(x/s)(h/r)$ (scatter advanced). Hence, the phase of the scattered component relative to the diffracted component is

$$\eta = 2\pi n[(x/s)(h/r) - (z/s)] = \alpha x - 2\pi n(z/s), \quad (\text{A1})$$

where $\alpha = 2\pi n h/rs$. Now define the amplitudes of the diffracted beam as a and the scattered light as b . The intensity resulting from interference between these two sources is given by

$$I = a^2 + b^2 + 2ab \cos \eta = I_0(1 + \epsilon \cos \eta), \quad (\text{A2})$$

where $I_0 = a^2 + b^2$ and $\epsilon = 2ab/(a^2 + b^2)$.

In the simple case of a diffracted beam of square profile, with intensity constant over a distance w along the meridian and zero elsewhere, Eq. A2 can be integrated over w to give the average intensity

$$\begin{aligned} \bar{I} &= (1/w) \int_{-w/2}^{w/2} I dx = (1/w) \{ I_0 x + (2ab/\alpha) \\ &\times [\cos(2\pi n z/s) \sin(\alpha x) - \sin(2\pi n z/s) \cos(\alpha x)] \} \Big|_{-w/2}^{w/2} \\ &= I_0 + (4ab/\alpha w) \cos(2\pi n z/s) \sin(\alpha w/2). \end{aligned} \quad (\text{A3})$$

The position of the centroid is

$$\bar{x} = \frac{\int_{-w/2}^{w/2} I x dx}{\int_{-w/2}^{w/2} I dx},$$

where the denominator is given above.

It can be shown that $\int_{-w/2}^{w/2} I x dx = (4ab/\alpha^2) \sin(2\pi n z/s) [\sin(\alpha w/2) - (\alpha w/2) \cos(\alpha w/2)]$ and

$$\bar{x} = \frac{(4ab/\alpha^2) \sin(2\pi n z/s) [\sin(\alpha w/2) - (\alpha w/2) \cos(\alpha w/2)]}{I_0 w + (4ab/\alpha) \cos(2\pi n z/s) \sin(\alpha w/2)}. \quad (\text{A4})$$

The maximum deviation of intensity from the average value I_0 occurs at $z = 0, s/2$:

$$d\bar{I} = I_0 \pm (4ab/\alpha w) \sin(\alpha w/2). \quad (\text{A5})$$

Similarly, the maximum deviation of the centroid from its mean position occurs at $z = \pm s/4$:

$$\begin{aligned} d\bar{x} &= \frac{\pm (4ab/\alpha^2) [\sin(\alpha w/2) - (\alpha w/2) \cos(\alpha w/2)]}{I_0 w} \\ &= \pm (2\epsilon/\alpha^2 w) [\sin(\alpha w/2) - (\alpha w/2) \cos(\alpha w/2)]. \end{aligned} \quad (\text{A6})$$

Equations A2–A6 generally are consistent with experiment. Equation A2 satisfactorily leads to a periodic intensity variation in x , and the spacing of these interference fringes at the first order agrees with the data of Figs. 5–7. The observed decrease in fringe spacing with increasing h is also explained. Equations A3 and A4 describe a variation in intensity and centroid with z (i.e., the fiber or grating is displaced), with n oscillations occurring for $\Delta z = s$, as observed. Equation A6 describes the amplitude of the centroid oscillation, and this decreases as h increases. This is in accordance with observation and is the result of the reduction in fringe spacing with an increase in h . The predicted amplitude of centroid oscillation and data of

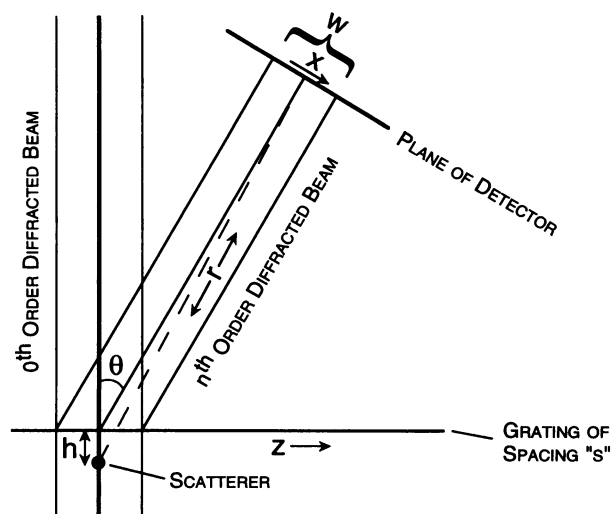


FIGURE 10 Diagram of interference between scattered and diffracted light. Light is incident from below on a grating representing a fiber. Light scattered from a point at a distance h below the grating interferes with light diffracted at angle θ into the diffraction order at a distance r from the scatterer. The other quantities are defined in the text.

Figs. 1 and 2 agree to within a factor of about two, but exact agreement is not to be expected for reasons given in the Discussion.

One obvious oversimplification of the theory is the square intensity profile of the diffracted beam. Therefore, we considered the effect of a Gaussian intensity profile, which approximately describes the diffraction order in the meridional direction. An observation apparently inconsistent with a purely Gaussian profile was the presence of strong interference fringes well away from the first order, where diffraction intensity and, therefore, fringe intensity should be insignificant. However, we note that part of the light scattered toward the fiber, $\sim 50\%$ in the case of the glass filament scatterer, is incident on the fiber over a continuous range of angles and itself will constitute a source of secondary diffraction continuous in θ . An estimate of the proportion of light diffracted into the first order can be taken from the work of Thornhill et al. (1991), who measured a first-order diffraction efficiency of 34% at the Bragg angle for a 71- μm -diameter fiber. This was consistent with 20–60% for fibers of 50–100 μm diameter expected from their theory; similar values are also expected on the theory of Sidick et al. (1992). For example, if the intensity of scattered light is 2.5% of the maximum at the center of the diffraction order ($b^2/a^2 = 0.025$), and assuming an efficiency of 40%, the secondary first-order light then would be $(0.5)(0.4)(2.5\%) = 0.5\%$ of the peak intensity of the primary first order. A Gaussian intensity profile and an approximate term for diffraction of scattered light were introduced into Eq. A2 by defining diffraction amplitude as

$$a_G = a e^{-(x^2/4\sigma^2)} + b\delta^{0.5}, \quad (\text{A7})$$

where a refers to the amplitude at the center of the beam, σ the SD of the Gaussian intensity profile, and δ the proportion of scattered light incident on the photodetector that is diffracted when a fiber is placed in the beam. Also, in Eq. A2 b is replaced by $b(1 - \delta)^{0.5}$. The term arising from scattered light is only approximate because it does not take into account variation in ϕ and diffraction efficiency with angle of incidence. Integration of intensity over x on and off the order to calculate \bar{I} and \bar{x} was done numerically, and examples of these calculations are shown in Fig. 9. The main result of this analysis is that the h dependence of centroid oscillation $d\bar{x}$ given in Fig. 9 E is nearly identical to the case of a beam of square profile (Eq. A4), except for the presence of alternating major and minor peaks at low h . These occur when the ratio of the fringe spacing to the order width is ~ 3 at $h \approx 0.1$ mm to about $1/3$ at $h \approx 0.6$ mm. However, the intensity oscillation with a Gaussian profile is predicted to be up to 10 times that with a square profile over the same range of h (Fig. 9 F); the two cases are similar at higher h . The measured intensity oscillations were intermediate between these two predictions. If the term in Eq.

A7 for light that is scattered and then diffracted is not included, fringe intensity becomes insignificant off the first order, and the oscillations in centroid vanish at h where the fringe spacing is much greater than the width of the order. Both predictions are inconsistent with experiment.

Several approximations made in deriving Eq. A1 were assessed by explicitly calculating the phase difference between the diffracted and scattered beams as a function of x , taking into account angle of incidence, wavelength, and size of the scatterer. In this case, \bar{x} , \bar{l} , and $d\bar{x}$ were calculated by numerical integration; $d\bar{x}$ and $d\bar{l}$ were then found by an iterative search on a fast computer. It was found that changes in angle of incidence or variation in ϕ of the diffracted light across the photodetector had little effect on the calculated fringe spacing (Fig. 9 A) or periodic maxima of $d\bar{x}$ vs. h (Fig. 9 E). The separation of the maxima and the phase of oscillations were however shifted. The small effect of these variables results from the low values of ϕ used ($1.22 \times 10^{-3} - 1.9^\circ$ for $\theta \leq 17^\circ$ and $r/h = 4000 - 30$ in the current experiments). In practice, experiments were done using various angles of incidence, and no significant change in the behavior of the oscillations was noted. In the derivation of Eq. A1, wavelength drops out because the dependence of η on λ is canceled by the dependence of θ on λ . The effect of λ was considered for three situations using the more exact numerical treatment: 1) the oscillations should be independent of wavelength if r is held constant as θ increases with λ ; 2) there also is no change in the maxima of $d\bar{x}$ if r is made to increase with λ (e.g., as occurs for a screen held parallel to the fiber); 3) if θ is made independent of λ , then the phase and spacing of the interference fringes are expected to depend on λ (larger spacing at higher λ). This effect would smear out the fringes and reduce the oscillation amplitude, consistent with the reduction in the size of oscillations in apparent sarcomere length during fiber shortening observed by Goldman (1987) using white light diffraction. A final potential complication that was considered was the effect of a diffuse scatterer, in contrast to the point scatterer of Fig. 10. It can be shown that the phase or spacing of interference fringes does not depend significantly on the position of scatterers within the ~ 1 -mm width of the laser beam, again because of the small value of ϕ .

REFERENCES

- Altringham, J. D., R. Bottinelli, and J. W. Lacktis. 1984. Is stepwise shortening an artefact? *Nature* 307:653-655.
- Baskin, R. J., R. L. Lieber, T. Oba, and Y. Yeh. 1981. Intensity of light diffraction from striated muscle as a function of incident angle. *Biophys. J.* 36:759-773.
- Brenner, B. 1985. Sarcomeric domain organization within single skinned rabbit psoas fibers and its effects on laser light diffraction patterns. *Biophys. J.* 48:967-982.
- Burton, K., and R. J. Baskin. 1986. Light diffraction patterns and sarcomere length variation in striated muscle fibers of *Limulus*. *Pflügers Arch.* 406:409-418.
- Burton, K., and A. F. Huxley. 1991. Identification of a source of oscillations in striation spacing estimated by laser diffraction during ramp shortening in muscle. *Biophys. J.* 59:46a. (Abstr.)
- Burton, K., W. N. Zagotta, and R. J. Baskin. 1989. Sarcomere length behaviour along single frog muscle fibres at different lengths during isometric tetani. *J. Muscle Res. Cell Motil.* 10:67-84.
- Cleworth, D. R., and K. A. P. Edman. 1972. Changes in sarcomere length during isometric tension development in frog skeletal muscle. *J. Physiol.* 227:1-17.
- Delay, M. J., N. Ishide, R. C. Jacobson, G. H. Pollack, and R. Tirosh. 1981. Stepwise sarcomere shortening: analysis by high-speed cinematography. *Science*. 213:1523-1525.
- Ellis, G. 1979. A fiber-optic phase-randomizer for microscope illumination by laser. *J. Cell Biol.* 83:303a. (Abstr.)
- Giilliar, W. G., W. S. Bickel, and W. F. Bailey. 1984. Light diffraction studies of single muscle fibers as a function of fiber rotation. *Biophys. J.* 45:1159-1165.
- Goldman, Y. E. 1987. Measurement of sarcomere shortening in skinned fibers from frog muscle by white light diffraction. *Biophys. J.* 52:57-68.
- Goldman, Y. E., and R. M. Simmons. 1984. Control of sarcomere length in skinned muscle fibres of *Rana temporaria* during mechanical transients. *J. Physiol.* 350:497-518.
- Goldspink, G., R. E. Larson, and R. E. Davies. 1970. Fluctuations in sarcomere length in the chick anterior and posterior latissimus dorsi muscles during isometric contractions. *Experientia*. 26:16-18.
- Granzier, H. L. M., and G. H. Pollack. 1985. Stepwise shortening in unstimulated frog skeletal muscle fibres. *J. Physiol.* 362:173-188.
- Hard, R., R. Zeh, and R. D. Allen. 1977. Phase-randomized laser illumination for microscopy. *J. Cell Sci.* 23:338-343.
- Huxley, A. F. 1984. Response to "Is stepwise shortening an artefact?" *Nature*. 309:713-714.
- Huxley, A. F. 1986. Comments on "Quantal mechanisms in cardiac contraction." *Circ. Res.* 59:9-14.
- Huxley, A. F. 1990. A theoretical treatment of diffraction of light by a striated muscle fibre. *Proc. R. Soc. Lond. B.* 241:65-71.
- Huxley, A. F., V. Lombardi, and L. D. Peachey. 1981a. A system for fast recording of longitudinal displacement of a striated muscle fibre. *J. Physiol.* 317:12-13.
- Huxley, A. F., V. Lombardi, and L. D. Peachey. 1981b. A system for recording sarcomere longitudinal displacements in a striated muscle fibre during contraction. *Boll. Soc. Ital. Biol. Sper.* 57:57-59.
- Jacobson, R. C., R. Tirosh, M. J. Delay, and G. H. Pollack. 1983. Quantized nature of sarcomere shortening steps. *J. Muscle Res. Cell Motil.* 4:529-542.
- Kawai, M., and I. D. Kuntz. 1973. Optical diffraction studies of muscle fibers. *Biophys. J.* 13:857-876.
- Lieber, R. L., Y. Yeh, and R. J. Baskin. 1984. Sarcomere length determination using laser diffraction. Effect of beam and fiber diameter. *Biophys. J.* 45:1007-1016.
- Paolini, P. J., R. Sabbadini, K. P. Roos, and R. J. Baskin. 1976. Sarcomere length dispersion in single skeletal muscle fibers and fiber bundles. *Biophys. J.* 16:919-930.
- Pollack, G. H., T. Iwazumi, H. E. D. J. ter Keurs, and E. F. Shibata. 1977. Sarcomere shortening in striated muscle occurs in stepwise fashion. *Nature*. 268:757-759.
- Pollack, G. H. 1986. Quantal mechanisms in cardiac contraction. *Circ. Res.* 59:1-8.
- Pollack, G. H., H. L. M. Granzier, A. Mattiazzi, C. Trombitás, A. Periasamy, P. H. W. Baatsen, and D. H. Burns. 1988. Pauses, steps, and the mechanism of contraction. In *Molecular Mechanism of Muscle Contraction*. H. Sugi and G. H. Pollack, editors. Plenum Publishing, New York. 617-637.
- Rüdel, R., and F. Zite-Ferenczy. 1979a. Interpretation of light diffraction by cross-striated muscle as Bragg reflection of light by the lattice of contractile proteins. *J. Physiol.* 290:317-330.
- Rüdel, R., and F. Zite-Ferenczy. 1979b. Do laser diffraction studies on striated muscle indicate stepwise sarcomere shortening? *Nature*. 278:573-575.
- Sidick, E., A. Knoesen, J. K. Xian, Y. Yeh, and R. J. Baskin. 1992. Rigorous analysis of light diffraction by a striated muscle fibre. *Proc. R. Soc. Lond. B.* 249:247-257.
- Sleep, J. 1989. Temperature control and exchange of the bathing solution for skinned muscle fibres. *J. Physiol.* 423:7P.
- Sundell, C. L., Y. E. Goldman, and L. D. Peachey. 1986. Fine structure in near-field and far-field laser diffraction patterns from skeletal muscle fibers. *Biophys. J.* 49:521-530.
- Thornhill, R. A., N. Thomas, and N. Berovic. 1991. Optical diffraction by well ordered muscle fibres. *Eur. Biophys. J.* 20:87-99.
- Yeh, Y., R. J. Baskin, R. L. Lieber, and K. P. Roos. 1980. Theory of light diffraction by single skeletal muscle fibers. *Biophys. J.* 29:509-522.
- Zite-Ferenczy, F., K. Häberle, R. Rüdel, and W. Wilke. 1986. Correlation between the light diffraction pattern and the structure of a muscle fibre realized with Ewald's construction. *J. Muscle Res. Cell Motil.* 7:197-214.